Monatshefte für Chemie 134, 489–499 (2003)
DOI 10.1007/s00706-002-0542-3

Monatshefte für Chemie
Chemical Monthly
Printed in Austria

Conformation and Crystal Structure of Dipyrrinones with Oxindole Components

Stefan E. Boiadjiev and **David A. Lightner***

Department of Chemistry, University of Nevada, Reno, Nevada 89557, USA

Received August 2, 2002; accepted August 30, 2002
Published online March 6, 2003

Summary. Pyrrole α-aldehydes (2-formyl-4,5-dimethyl-1*H*-pyrrole and 2-formyl-*N*-methylpyrrole) condense readily at C(3) of indolin-2-ones to give dipyrrinone analogs, such as (3*Z*)-[(4,5-dimethyl-pyrrol-2-yl)-methylidenyl]-indolin-2-one and (3*E*)-[(1-methylpyrrol-2-yl)-methylidenyl]-indolin-2-one. ^{1}H-NMR N*O*E analyses and X-ray crystallography confirm the *syn*-(*Z*) configuration for the former and the *syn*-(*E*) configuration for the latter. The former is stabilized by intramolecular hydrogen bonding. Molecular mechanics calculations of the latter indicate no energy difference between the *syn* and *anti* conformations.

Keywords. Pyrrole; X-ray structure; Hydrogen bonding.

Introduction

Our interest in synthetic bile pigments with aromatic substituents [1–3] and annelated pyrrole rings led us to prepare and investigate potential dipyrrinone synthons for the latter. Two types of potential precursors are oxisoindole and oxindole, with the former leading to the conventional bile pigment types. The latter condenses easily with pyrrole α-aldehydes, reactions that formed the basis for a study of antiangiogenic agents targetting at receptor tyrosine kinases [4–6]. In the following we describe the synthesis of a new potential antiangiogenic agent **1** (Fig. 1) from 2-indolinone (**3**) and compare its conformation to that of a known analog **2** using N*O*E NMR spectroscopy and X-ray crystallography.

Results and Discussion

Synthesis

3-[(Pyrrol-2-yl)-methylidenyl]-indolin-2-ones **1** and **2** were prepared in excellent yields by piperidine-catalyzed condensation of **3** with 2-formyl-4,5-dimethylpyrrole

* Corresponding author. E-mail: lightner@scs.unr.edu

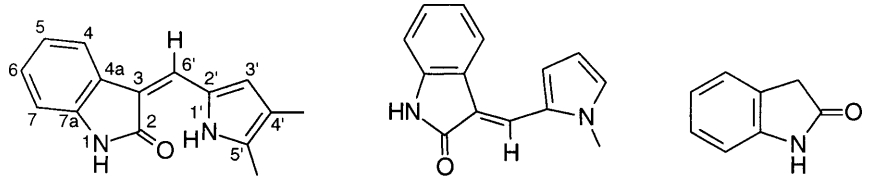

1 **2** **3**

Fig. 1. 3-[(4′,5′-dimethylpyrrol-2-yl)-methylidenyl]-indolin-2-one (**1**) and 3-[(*N*-methylpyrrol-2-yl)-methylidenyl]-indolin-2-one (**2**) and 2-oxindole (**3**), with numbering system consistent with Ref. [4]

(**4**) [7] and *N*-methylpyrrole-2-aldehyde (**5**), respectively, in refluxing methanol (Scheme 1). The pyrrole aldehydes were prepared by *Vilsmeier* formylation of 2,3-dimethylpyrrole and *N*-methylpyrrole [8]. The former was synthesized from benzyl 4,5-dimethylpyrrole-2-carboxylate.

Constitution and Conformation in Solution

The constitutional structures of **1** and **2** follow from the method of synthesis and their NMR spectra (Table 1). The signal assignments of Table 1 were secured by gHMQC and gHMBC NMR experiments. Compound **2** has been reported previously [4] to adopt an (*E*)-configuration of the exocyclic carbon–carbon double bond to alleviate an unfavorable intramolecular steric buttressing between the N–CH_3 and the carbonyl group in the (*Z*)-configuration isomer. The (*E*)-configuration of **2** is confirmed by N*O*Es seen between the aromatic ring 4-H and the pyrrole 3′-H, and the *syn*-conformation is confirmed by an N*O*E between 6′-H and the N–CH_3. In the *anti*-(*Z*) configuration, which is favored in **6** [9], one would expect an N*O*E between 4-H and 6′-H, which is not seen in **2**.

The (*Z*)-configuration of **1** is confirmed by N*O*Es between 4-H and 6′-H, and its *syn*-conformation is confirmed by N*O*Es between the 6′-H and 3′-H. But very weak N*O*Es between the 6′-H and the pyrrole NH suggest the presence of some *anti* diastereomer. Other N*O*Es are shown in Fig. 2 by double-headed curved arrows.

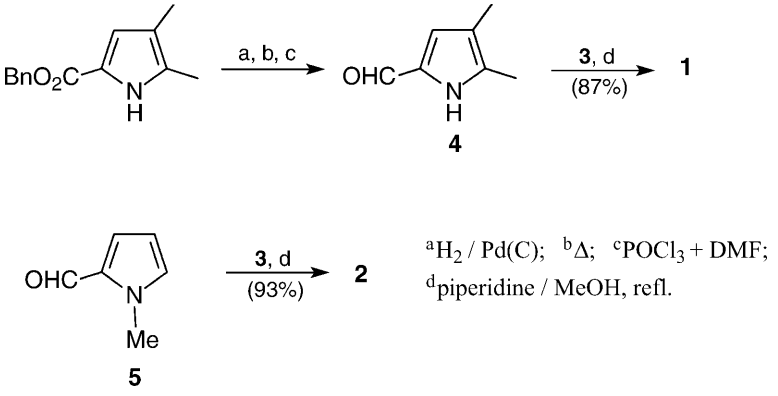

4 **5**

Scheme 1

Table 1. Proton and carbon NMR assignments of **1** and **2** in $CDCl_3$ at 25°C

	1		**2**	
	δ_C/ppm	δ_H/ppm	δ_C/ppm	δ_H/ppm
2-CO	169.50	–	171.15	–
3	113.02	–	121.35	–
4a	126.32	–	122.49	–
4	117.57	7.45	122.40	8.12
5	121.62	7.04	121.66	6.99
6	125.76	7.13	128.65	7.21
7	109.22	6.89	109.91	6.92
7a	137.05	–	140.73	–
2′	127.93	–	128.49	–
3′	122.67	6.56	116.02	7.15
4′	120.28	–	109.67	6.34
5′	135.44	–	127.72	6.89
6′	126.16	7.30	124.23	7.63
N–CH_3	–	–	34.61	3.81
4′-CH_3	10.83	2.08	–	–
5′-CH_3	12.19	2.34	–	–
CONH	–	7.84	–	8.48
pyr NH	–	13.06	–	–

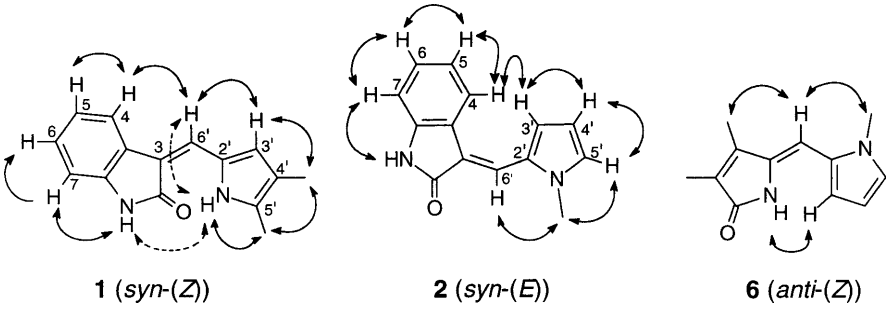

Fig. 2. N*O*Es observed for **1** and **2** in $CDCl_3$ solvent are shown by solid arrows. Weak N*O*Es are shown by dashed arrows. The N*O*Es observed for **2** are consistent with the (*E*)-configuration

The unusually deshielded proton on the pyrrole nitrogen of **1** (Table 1) suggests strong hydrogen bonding, presumably to the lactam carbonyl. In **2** the 4-H is unusually deshielded (8.12 ppm) compared to **1** (7.45 ppm), but the remaining aromatic hydrogens all have rather similar chemical shifts (6.89–7.21 ppm). Interestingly, the aromatic ring carbons show an alternating effect of the (*Z*) or (*E*) configuration, with carbons 5 (121.62, 121.66 ppm) and 7 (109.22, 109.91 ppm) exhibiting similar chemical shifts, but carbons 4 (117.57, 122.40 ppm), 6 (125.76, 128.65 ppm), and 7a (137.05, 140.73 ppm) showing 3–5 ppm greater deshielding in **2** than in **1**.

Molecular Structure in the Crystal

Except for an X-ray crystal structure of 3-[(3-(2-carboxyethyl)-4-methylpyrrol-2-yl)-methylidenyl]-2-indolinone located in the tyrosine kinase domain of fibroblast growth factor receptor [6], crystal structures of 3-[(pyrrol-2-yl)-methylidenyl]-2-indolinones appear to be absent. On the protein, the pigment is found to adopt a *syn*-(*Z*) configuration [6].

Single crystals of **1** and **2** were grown from dichloromethane-methanol and from diffusion of *n*-hexane vapor into dichloromethane-ethyl acetate, respectively. In (yellow) crystals of **1**, the C(1)–C(4)–C(5)–C(6) = -1.8° and C(4)–C(5)–C(6)–N(2) = -1.5° torsion angles are both close to zero, which means the molecules

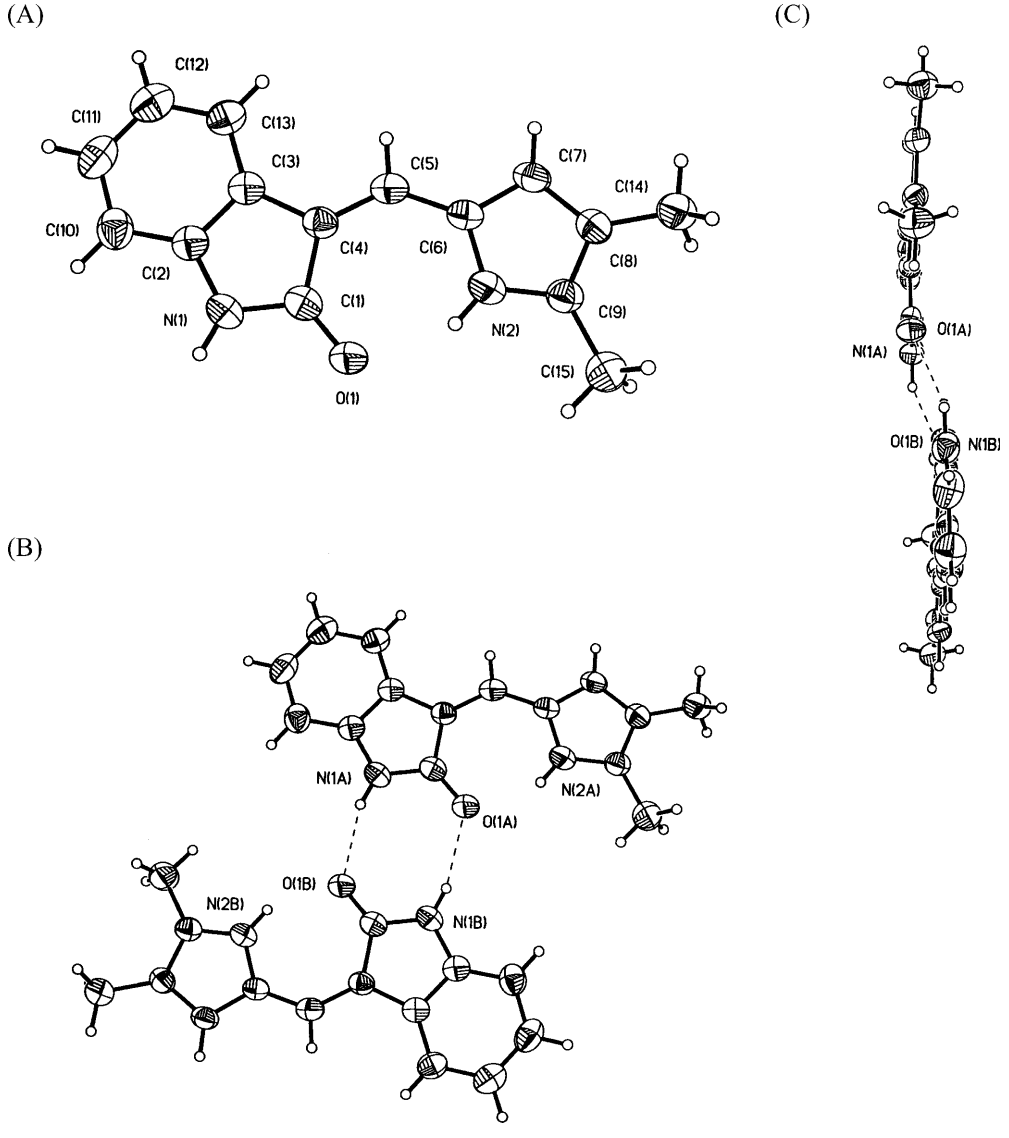

Fig. 3. (A) Crystal structure of **1**, top view, with crystal structure numbering used. Top (B) and edge (C) views of the dimer of **1** found in the crystal. The thermal ellipsoids represent 40% occupancy

(Fig. 3) are planar and adopt the *syn*-(*Z*) configuration. The nonbonded distance between the pyrrole N–H and lactam carbonyl oxygen is only 1.919 Å, suggesting very strong intramolecular hydrogen bonding. Longer intermolecular hydrogen

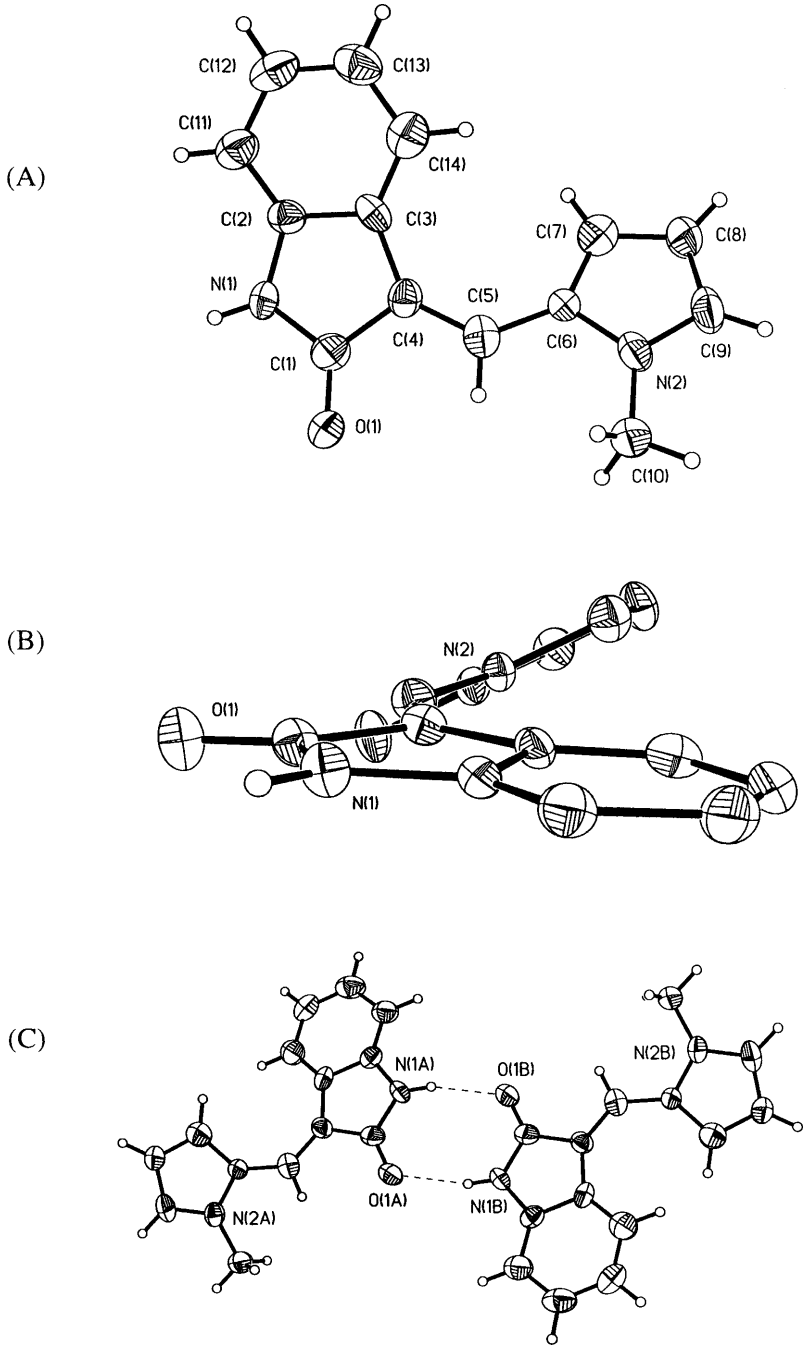

Fig. 4. Crystal structure of **2**, top view (A), with crystal numbering used, and (B) side view showing nonplanarity of the molecule. (C) Top view of hydrogen-bonded dimer of **2** found in the crystal. The thermal ellipsoids represent 40% occupancy (20% in (B)

bonds between the lactam groups are suggested by the nonbonded distances, but the two molecules of the hydrogen-bonded pair are not co-planar (Fig. 3B and C). The dominant factor in stabilizing the *syn*-conformation in the crystal and in solution appears to be the strong intramolecular hydrogen bond between the pyrrole NH and lactam C=O.

Unlike **1**, the crystal structure (Fig. 4) of **2** (yellow plates) confirms the *syn*-(*E*) configuration and shows the molecule to be twisted about the middle, mainly in the C(5)–C(6) single bond, with torsion angle C(4)–C(5)–C(6)–C(7) = $-25.3°$. Very little twisting is observed in the exocyclic carbon–carbon double bond: C(3)–C(4)–C(5)–C(6) = $-9.3°$. Like **1**, dipyrrinone **2** forms lactam to lactam hydrogen-bonded dimers in the crystal, where enantiomeric conformations pair up.

Intramolecular hydrogen bonding may account for the slightly longer C=O bond length in **1** (1.249 Å) *vs.* that of **2** (1.229 Å) and a wider N(2)–C(6)–C(5) bond angle in **1** (125.1°) *vs.* that of **2** (121.9°). However, the choice of (*Z*) or (*E*) configuration at C(4)–C(5) does not result in much change in this bond length, nor in the C(5)–C(6) bond length, and most bond lengths and angles in **1** and **2** are comparable.

Conformational Analysis by Molecular Mechanics Calculations

Computations using PCModel [10a] and Sybyl [10b] show that the *syn-Z* configuration of **1** is planar and favored over the *anti* rotamer by 13.8–32.2 kJ mol^{-1} (Table 2). The larger relative total energy found in Sybyl is probably due to an overestimation of stabilization by hydrogen bonding. In **2**, the *syn* and *anti* (*E*)-isomers are nearly isoenergetic; yet, the N*O*E data and X-ray crystallographic study clearly indicates a preference for the *syn* conformation in solution and in the solid state. Also, the torsion angle from X-ray crystallography of **2** is less (25°) than that found by molecular mechanics (80°). Possibly, crystal packing forces come into play to stabilize the more planar conformation of the *syn* conformation and shrink the torsion angle.

UV-Visible Spectral Characteristics

The long-wavelength UV-visible maximum absorbance of **1** is significantly shifted to longer wavelengths than that of **2** in all solvents studied. For the former, solvent

Table 2. Computed[a] torsion angles ° and relative energies for the *syn* and *anti* conformations of **1** and **2**

	1			**2**	
	3-6′-2′-1′ (4-5-6-N)/deg	Relative total E^b/kJ mol^{-1}		3-6′-2′-1′ (4-5-6-N)/deg	Relative total E^b/kJ mol^{-1}
syn-(*Z*)	0.1°	0.0	*syn*-(*E*)	80.4°	0.4
	− 0.2°	*0.0*		*80.4°*	*0.0*
anti-(*Z*)	108.0°	13.8	*anti*-(*E*)	− 81.8°	0.0
	108.2°	*32.2*		*− 58.2°*	*0.0*

[a] Values using the MMX force field of PCModel v7.5 [10a] and *in italics* from Tripos' Sybyl [10b];
[b] relative *E* = total *E* (*anti*) − total *E* (*syn*)

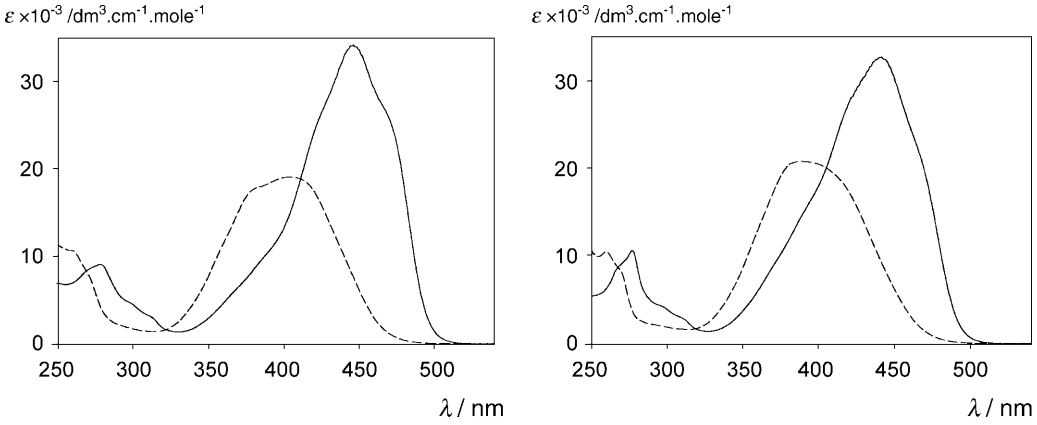

Fig. 5. UV-Vis spectra of $10^{-5}M$ **1** (—) and **2** (– – – –) in chloroform (left) and methanol (right) at 23°C

influence on λ_{max} and ε_{max} is relatively small (Fig. 5). Thus, **1** exhibits λ_{max} at 445 nm ($\varepsilon = 34{,}200$) in $CHCl_3$ solvent and λ_{max} at 444 nm ($\varepsilon = 31{,}600$) in *DMSO*. In contrast, **2** exhibits λ_{max} 404 ($\varepsilon = 19{,}100$) in $CHCl_3$ and λ_{max} at 381 ($\varepsilon = 19{,}400$) in *DMSO*. The ~50 nm longer λ_{max} of **1** (relative to **2**) is presumably due to the more extended and flattened chromophore of the former.

Experimental

All NMR spectra were obtained on a Varian Unit Plus spectrometer operating at ^1H frequency of 500 MHz in $CDCl_3$ solvent. Chemical shifts are reported in δ (ppm) referenced to the residual $CHCl_3$ ^1H signal at 7.26 ppm, and $CDCl_3$ ^{13}C signal at 77.00 ppm. A *J*-modulated spin-echo experiment (*A*ttached *P*roton *T*est) as well as 2D HETCOR, gHMQC and gHMBC spectra were used to assign the ^1H and ^{13}C-NMR spectra. UV-visible spectra were measured on a Perkin-Elmer lambda-12 spectrophotometer. Melting points were taken on a Mel-Temp capillary apparatus and are uncorrected. Gas chromatography-mass spectrometry analyses were carried out on a Hewlett-Packard 5890A capillary gas chromatograph (30 m DB-1 column) equipped with Hewlett-Packard 5970 mass selective detector. Radial chromatography was carried out on Merck silica gel PF_{254} with $CaSO_4$ binder, preparative layer grade, using a chromatotron (Harrison Research, Inc., Palo Alto, CA). Combustion analyses were carried out by Desert Analytics, Tucson, AZ. The experimental values were within $\pm 0.3\%$ of the calculated values. Commercial reagents and HPLC grade solvents were dried and purified following standard procedures [11]. Oxindole and piperidine were from ACROS. Benzyl 4,5-dimethyl-1*H*-pyrrole-2-carboxylate [12], 2,3-dimethyl-1*H*-pyrrole [7c]. 4,5-dimethyl-2-formyl-1*H*-pyrrole (**4**) ([7a, b] adapted from [13]) and 2-formyl-*N*-methylpyrrole (**5**) [8] were synthesized according to literature procedures.

(3Z)-[(4,5-Dimethylpyrrol-2-yl)-methylidenyl]-indolin-2-one (**1**, $C_{15}H_{14}N_2O$)

A mixture of 616 mg (5.00 mmol) of 4,5-dimethyl-2-formyl-1*H*-pyrrole (**4**) [7, 13], 533 mg (4.00 mmol) of oxindole, 0.21 cm^3 (2.00 mmol) of piperidine, and 25 cm^3 of anh. methanol was heated at reflux for 8.5 h. After cooling the mixture was chilled overnight at $-15°$. Then the precipitated product was collected by filtration and washed with cold CH_3OH. Purification by radial chromatography (eluting with CH_2Cl_2–CH_3OH = 100:2 to 100:4) and recrystallization from CH_2Cl_2–CH_3OH afforded pure bright yellow-orange **1**. Yield 829 mg (87%); mp 271–272°C; ^1H-NMR and ^{13}C-NMR

data in Table 1; UV/vis (C_6H_6): $\lambda_{sh} = 468$ (24700), $\lambda_{max} = 444$ (34100), $\lambda_{sh} = 423$ (26600); (CH_3OH): $\lambda_{sh} = 465$ (22100), $\lambda_{max} = 439$ (32500), $\lambda_{sh} = 420$ (27900), $\lambda_{max} = 276$ (9700) nm (ε).

(3E)-[(1-Methylpyrrol-2-yl)-methylidenyl]-indolin-2-one (**2**, $C_{14}H_{12}N_2O$)

Following the procedure above, **2** was synthesized from 533 mg (4.00 mmol) of oxindole and 655 mg (6.00 mmol) of 2-formyl-*N*-methylpyrrole (**5**) [8]. After chromatography, the material was recrystallized from CH_2Cl_2–CH_3OH to afford bright yellow **2** [4]. Yield 834 mg (93%); mp 216–217°C; ^{1}H-NMR and ^{13}C-NMR data in Table 1; UV/vis (C_6H_6): $\lambda_{max} = 404$ (18200), $\lambda_{max} = 379$ (17700); (CH_3OH): $\lambda_{sh} = 403$ (20200), $\lambda_{max} = 389$ (20800) nm (ε).

Table 3. Crystal data and structure refinement for **1** and **2**

	1	**2**
Formula weight	238.28	224.26
Crystallized from	CH_2Cl_2/CH_3OH	CH_2Cl_2/ethyl acetate, *n*-hexane diffusion
Temperature	298(2) K	298(2) K
Formula	$C_{15}H_{14}N_2O$	$C_{14}H_{12}N_2O$
Crystal size [mm]	0.40×0.40×0.08	0.45×0.22×0.08
Crystal system	monoclinic	orthorhombic
Space group	P2(1)/n	Pbca
Z	4	8
Unit cell dimensions	$a = 12.1011(16)$ Å $\alpha = 90°$ $b = 6.3689(18)$ Å $\beta = 102.374(16)°$ $c = 16.333(4)$ Å $\gamma = 90°$	$a = 14.231(3)$ Å $\alpha = 90°$ $b = 7.5238(19)$ Å $\beta = 90°$ $c = 21.770(4)$ Å $\gamma = 90°$
Volume	1229.6(5) Å^3	2330.9(8) Å^3
Density (calculated)	1.287 Mg/m^3	1.278 Mg/m^3
Absorption coefficient	0.082 mm^{-1}	0.082 mm^{-1}
F(000)	504	944
Crystal habit and color	plate, yellow	plate, yellow
Theta range for data collection	1.91° to 29.79°	1.87 to 22.51°
Index ranges	$-1 \le h \le 14$, $-8 \le k \le 1$, $-19 \le l \le 19$	$-15 \le h \le 15$, $-8 \le k \le 1$, $-23 \le l \le 23$
Reflections collected	2985	6882
Independent reflections	2174 [R(int) = 0.0313]	1523 [R(int) = 0.1498]
Completeness to theta = 29.79° (**1**); 22.51° (**2**)	52.4%	82.0%
Absorption correction	empirical	empirical
Max. and min. transmission	0.9102 and 0.8771	0.9670 and 0.8741
Refinement method	full-matrix least-squares on F^2	full-matrix least-squares on F^2
Data/restraints/parameters	2174/0/164	1523/0/155
Goodness-of-fit on F^2	1.020	1.024
Final R indices [$I > 2$sigma(I)]	$R1 = 0.0596$, $wR2 = 0.1250$	$R1 = 0.0642$, $wR2 = 0.1073$
R indices (all data)	$R1 = 0.1288$, $wR2 = 0.1539$	$R1 = 0.1743$, $wR2 = 0.1420$
Largest diff. peak and hole	0.239 and -0.159 e Å^{-3}	0.219 and -0.196 e Å^{-3}

X-Ray Structure and Solution

Yellow-orange crystals of **1** were grown in CH_2Cl_2–CH_3OH. A suitable crystal ($0.40\times0.40\times0.08$ mm) was mounted on a glass fiber, coated with epoxy and placed on the goniometer of a Siemens P4 diffractometer. Unit cell parameters were determined by least squares analysis of 28 reflections with $5.1^\circ<\theta<11.7^\circ$ using graphite monochromatized MoKα radiation ($\lambda=0.71073$ Å). A total of 2985 reflections were collected between $3.8^\circ<2\theta<59.7^\circ$ yielding 2174 unique reflections ($R_{int}=0.0313$). The data were corrected for *Lorentz*, polarization effects and absorption using an empirical model derived from psi scans. Crystal data are presented in Table 3. Scattering factors and corrections for anomalous dispersion were taken from a standard source [14]. Calculations were performed with Siemens SHELXTL Plus (v 5.1) software package [15]. The structure was solved by direct methods in space group P2(1)/n.

Long yellow plates of **2** were grown by *n*-hexane vapor diffusion into CH_2Cl_2-ethyl acetate solution. A crystal, after cutting to size $0.45\times0.22\times0.08$ mm, was manipulated as above. Unit cell was determined by least squares analysis of 24 reflections with $4.7^\circ<\theta<9.9^\circ$ and data collection and analysis proceeded as described above for **1**. Crystal data for **2** are given in Table 3. The structure was solved by direct methods in P_{bca} space group.

All non-hydrogen atoms were refined with anisotropic thermal parameters. Hydrogen atoms were placed at ideal positions calculated using a riding model with a C–H distance fixed at 0.96 Å and a thermal parameter 1.2 times the host atoms. The structures were refined by the full-matrix least squares method on F^2. The final refinement converged to $R1=0.0596$, $wR2=0.1250$ for **1**; $R1=0.0642$, $wR2=0.1073$ for **2** and goodness-of-fit: 1.020 and 1.024, respectively. Tables 4 and 5 provide atomic coordinates for **1** and **2**, respectively.

Tables of anisotropic displacement parameters, isotropic displacement parameters, atomic coordinates, bond angles and lengths for **1** and **2** have been deposited at the Cambridge Crystallographic Data Center (CCDC No. 190066 for **1** and 190067 for **2**).

Table 4. Atomic coordinates ($\times10^4$) and equivalent isotropic displacement parameters (Å$^2\times10^3$) for **1**. *U*(eq) is defined as one third of the trace of the orthogonalized U^{ij} tensor

	x	*y*	*z*	*U*(eq)
N(1)	956(2)	2953(4)	− 293(2)	54(1)
N(2)	766(2)	1299(4)	2379(2)	53(1)
O(1)	516(2)	3641(3)	985(1)	57(1)
C(1)	916(2)	2446(5)	515(2)	47(1)
C(2)	1441(2)	1355(5)	− 680(2)	49(1)
C(3)	1740(2)	− 275(5)	− 106(2)	46(1)
C(4)	1420(2)	335(5)	673(2)	45(1)
C(5)	1525(2)	− 873(5)	1380(2)	50(1)
C(6)	1234(2)	− 515(5)	2157(2)	47(1)
C(7)	1326(2)	− 1870(5)	2837(2)	52(1)
C(8)	898(3)	− 869(5)	3458(2)	50(1)
C(9)	543(3)	1105(5)	3151(2)	50(1)
C(10)	1615(3)	1259(6)	− 1484(2)	62(1)
C(11)	2133(3)	− 525(7)	− 1705(2)	72(1)
C(12)	2447(3)	− 2170(7)	− 1146(2)	72(1)
C(13)	2250(3)	− 2048(6)	− 342(2)	57(1)
C(14)	806(3)	− 1720(6)	4302(2)	65(1)
C(15)	8(3)	2837(6)	3544(2)	73(1)

Table 5. Atomic coordinates ($\times 10^4$) and equivalent isotropic displacement parameters ($Å^2 \times 10^3$) for **2**. U(eq) is defined as one third of the trace of the orthogonalized U^{ij} tensor

	x	y	z	U(eq)
N(1)	4335(3)	2086(6)	4964(2)	48(1)
N(2)	4062(3)	3931(6)	2297(2)	47(1)
O(1)	4814(3)	263(6)	4173(2)	63(1)
C(1)	4447(4)	1644(9)	4356(3)	50(2)
C(2)	3952(3)	3791(7)	5030(3)	45(1)
C(3)	3780(4)	4460(8)	4436(3)	44(2)
C(4)	4071(4)	3131(8)	3992(2)	43(2)
C(5)	4100(4)	2982(8)	3368(2)	54(2)
C(6)	3735(4)	4045(7)	2898(2)	40(1)
C(7)	2986(4)	5229(8)	2867(2)	63(2)
C(8)	2870(4)	5805(8)	2269(2)	62(2)
C(9)	3558(4)	4975(8)	1927(2)	60(2)
C(10)	4859(4)	2851(8)	2106(2)	65(2)
C(11)	3764(4)	4688(9)	5562(3)	60(2)
C(12)	3401(4)	6418(9)	5502(3)	71(2)
C(13)	3261(4)	7122(8)	4928(3)	67(2)
C(14)	3444(4)	6156(9)	4398(3)	61(2)

Acknowledgments

We thank the U.S. National Institutes of Health (HD 17779) for generous support of this research. Dr. *S.E.B.* is on leave from the Institute of Organic Chemistry, Sofia, Bulgaria. We thank Dr. *G.B. Quistad* for preparing the *N*-methyl-2-pyrrole aldehyde used in this work. Special thanks are accorded to Profs. *J. Nelson* and *V.J. Catalano* for helpful discussions on the X-ray crystallographic determinations.

References

[1] Brower JO, Lightner DA, McDonagh AF (2001) Tetrahedron **57**: 7813
[2] Brower JO, Lightner DA (2001) Monatsh Chem **12**: 1527
[3] Boiadjiev SE, Lightner DA (2002) Tetrahedron **58**: 7411
[4] Sun L, Tran N, Tang F, App H, Hirth P, McMahon G, Tang C (1998) J Med Chem **41**: 2588
[5] a) Sun L, Tran N, Liang C, Hubbard S, Tang F, Lipson K, Schreck R, Zhou Y, McMahon G, Tang C (2000) J Med Chem **43**: 2655; b) Sun L, Tran N, Liang C, Tang F, Rice A, Schreck R, Waltz K, Shawver LK, McMahon G, Tang C (1999) J Med Chem **42**: 5120
[6] Mohammadi M, McMahon G, Sun L, Tang C, Hirth P, Yeh BK, Hubbard SR, Schlessinger J (1997) Science **276**: 955
[7] a) Corwin AH, Krieble RH (1941) J Am Chem Soc **63**: 1829; b) Fischer H, Orth H (1934) Die Chemie des Pyrrols, Bd I, Akademische Verlagsgesellschaft MbH, Leipzig, 54; c) *ibid*, 41
[8] Lightner DA, Quistad GB (1973) J Heterocyclic Chem **10**: 273
[9] Cullen DL, Pèpe G, Meyer EF Jr, Falk H, Grubmayer K (1979) J Chem Soc Perkin Trans II: 999
[10] a) PC Model version 7.5, Serena Software, Bloomington, IN USA; b) Sybyl version 6.4, Tripos Assoc, St. Louis, MO USA
[11] Perrin DD, Armarego WLF (1988) Purification of Laboratory Chemicals, 3rd ed Pergamon Press, England

[12] Budzikiewicz H, Djerassi C, Jackson AH, Kenner GN, Newman DJ, Wilson JM (1964) J Chem Soc 1949
[13] deLeon CY, Ganem B (1997) Tetrahedron **53**: 7731
[14] Ibers JA, Hamilton WC (1974) International Tables for X-ray Crystallography, vol 4, Kynoch Press, Birmingham England
[15] SHELXTL-Plus, v 5.1, Bruker Analytical X-ray Systems, Madison, WI USA